Supplement of Atmos. Chem. Phys., 21, 9681–9704, 2021
https://doi.org/10.5194/acp-21-9681-2021-supplement

Atmospheric Chemistry and Physics
Open Access

Supplement of

Highly oxygenated organic molecule (HOM) formation in the isoprene oxidation by NO_3 radical

Defeng Zhao et al.

Correspondence to: Thomas F. Mentel (t.mentel@fz-juelich.de) and Defeng Zhao (dfzhao@fudan.edu.cn)

In the supplement we describe the derivation of calibration coefficient of NO_3^--CIMS for H_2SO_4. In addition, more tables and figures besides those in the main text are provided.

1 S1 Deriving calibration coefficient of H_2SO_4 in NO_3^--CIMS and HOM yield

In order to convert peak intensity in mass spectra to concentration, the calibration coefficient of H_2SO_4 is derived. H_2SO_4 was produced in-situ in SAPHIR chamber by the oxidation SO_2 by OH. SO_2 (~15 ppb) was added into the chamber and the roof was opened to initiate photo-oxidation. In SAPHIR chamber, OH radicals are mainly formed by the photolysis of HONO (nitrous acid) directly coming off the chamber walls through a photolytic process (Rohrer et al., 2005;Zhao et al., 2016). NO (~20 ppb) was added which can enhance OH production by photochemical recycling. OH concentration was characterized by using laser induced fluorescence (LIF) with the details described in (Fuchs et al., 2012). SO_2 concentrations was characterized using an SO_2 analyzer (Thermo Systems 43i).

The concentration of H_2SO_4 in the chamber can be described by the following equation.

$$\frac{d[H_2SO_4]}{dt} = k[SO_2][OH] - (k_{wl} + k_{dil})[H_2SO_4]) \quad \text{(Eq. 1)}$$

where $[H_2SO_4]$, $[SO_2]$, [OH] are the concentration of these species, k is the rate constant for the reaction of SO_2 with OH, k_{wl} is the wall loss rate of H_2SO_4 (~6.0×10^{-4} s^{-1} as characterized for low volatility compounds in our previous publication (Zhao et al., 2018)) and k_{dil} is the dilution rate of H_2SO_4 (~1×10^{-5} s^{-1}).

$$[H_2SO_4]=C\times I \quad \text{(Eq. 2)}$$

where C is the calibration coefficient of H_2SO_4, I is the peak intensity of H_2SO_4 determined by normalized peak area of H_2SO_4 at time t, i.e., the peak area divided by total signal of mass spectrum (termed as normalized count (nc)).

Substituting Eq.2 to Eq. 1, one can get

$$C\frac{dI}{dt} = k[SO_2][OH] - C(k_{wl} + k_{dil})I \quad \text{(Eq. 3)}$$

Integrating Eq.3, one can get

$$C = \frac{k[SO_2][OH]}{\frac{I-I_0}{t}+(k_{wl}+k_{dil})I} \quad \text{(Eq. 4)}$$

where I_0 is the peak intensity at time zero. C was determined to be 2.5×10^{10} molecules cm^{-3} nc^{-1}. The second term of denominator in Eq. 4 is much lower the first term and can omitted. The uncertainty of C was estimated to -52%/+ 101% from the uncertainty of SO_2 concentration (~7 %), OH concentration (~ 10 %), I (~ 10%) and k (Δlogk=±0.3) using error propagation, which corresponds to (1.2-5.0)$\times10^{10}$ molecules cm^{-3} nc^{-1}. The C value is generally consistent with the value of 3.7×10^{10} molecules cm^{-3} nc^{-1} in our previous calibration (Pullinen et al., 2020).

HOM yield was calculated as

$$Y = \frac{[HOM]}{[VOC]_r} = \frac{I(HOM)C}{[VOC]_r} \quad \text{(Eq. 5)}$$

where [HOM] is concentration of HOM and $[VOC]_r$ is the concentration of VOC reacted. The uncertainty of HOM yield was estimated to -55%/+ 103% from the uncertainty of HOM intensity (~10 %), VOC concentration (~ 15 %) and C using error propagation.

2 S2 Detailed mechanisms of trimer formation

The $C_{15}H_{25}N_5O_n$ series can be formed by the following reactions:

$$C_{10}H_{16}N_3O_{n1}\bullet + C_5H_9N_2O_{n2}\bullet \rightarrow C_{15}H_{25}N_5O_{n1+n2-2} + O_2 \quad \text{RS1}$$

$$C_{10}H_{17}N_4O_{n1}\bullet + C_5H_8NO_{n2}\bullet \rightarrow C_{15}H_{25}N_5O_{n1+n2-2} + O_2 \quad \text{RS2}$$

$$C_{10}H_{18}N_3O_{n1}\bullet + C_5H_7N_2O_{n2}\bullet \rightarrow C_{15}H_{25}N_5O_{n1+n2-2} + O_2 \quad \text{RS3}$$

The $C_{10}H_{18}N_3O_n$ (n=14-20) and $C_{10}H_{17}N_4O_n$ can be formed by the dimers with NO_3.

$$C_{10}H_{18}N_2O_n + NO_3 + O_2 \rightarrow C_{10}H_{18}N_3O_n\bullet \quad \text{RS4}$$

$$C_{10}H_{17}N_3O_n + NO_3 + O_2 \rightarrow C_{10}H_{17}N_4O_n \quad \text{RS5}$$

R21 is likely to be unimportant because both the abundance of $C_{10}H_{18}N_3O_n$ and $C_5H_7N_2O_n$ were low. Since the peaks of $C_{10}H_{18}N_3O_n$ (n=14-20) series overlap with $C_{10}H_{16}N_2O_n$, we can only assign them with low confidence. Similarly, $C_{10}H_{17}N_4O_n$ series overlap with $C_{10}H_{15}N_3O_n$ series (dimer 5).

The $C_{15}H_{25}N_3O_n$ series can be formed by the following reactions:

$$C_{10}H_{17}N_2O_{n1}\bullet + C_5H_8NO_{n2}\bullet \rightarrow C_{15}H_{25}N_3O_{n1+n2-2} + O_2 \quad \text{RS6}$$

$$C_{10}H_{16}NO_{n1}\bullet + C_5H_9N_2O_{n2}\bullet \rightarrow C_{15}H_{25}N_3O_{n1+n2-2} + O_2 \quad \text{RS7}$$

The $C_{15}H_{26}N_4O_n$ series can be formed by the following reactions:

$$C_{10}H_{17}N_2O_{n1}\bullet + C_5H_9N_2O_{n2}\bullet \rightarrow C_{15}H_{26}N_4O_{n1+n2-2} + O_2 \quad \text{RS8}$$

$$C_{10}H_{18}N_3O_{n1}\bullet + C_5H_8NO_{n2}\bullet \rightarrow C_{15}H_{26}N_4O_{n1+n2-2} + O_2 \quad \text{RS9}$$

$$C_{10}H_{16}N_3O_{n1}\bullet + C_5H_{10}NO_{n2}\bullet \rightarrow C_{15}H_{26}N_4O_{n1+n2-2} + O_2 \quad \text{RS10}$$

R28 is likely to be unimportant because both the abundance of $C_{10}H_{16}N_3O_n$ and $C_5H_{10}NO_n$ were low.

The $C_{15}H_{24}N_2O_n$ series can be formed by the following reactions:

$$C_{10}H_{16}NO_{n1}\bullet + C_5H_8NO_{n2}\bullet \rightarrow C_{15}H_{24}N_2O_{n1+n2-2} + O_2 \quad \text{RS11}$$

$C_{10}H_{16}NO_{n1}\bullet$ is formed via R15 as mentioned above.

References:

Fuchs, H., Dorn, H. P., Bachner, M., Bohn, B., Brauers, T., Gomm, S., Hofzumahaus, A., Holland, F., Nehr, S., Rohrer, F., Tillmann, R., and Wahner, A.: Comparison of OH concentration measurements by DOAS and LIF during SAPHIR chamber experiments at high OH reactivity and low NO concentration, Atmos. Meas. Tech., 5, 1611-1626, 10.5194/amt-5-1611-2012, 2012.

Pullinen, I., Schmitt, S., Kang, S., Sarrafzadeh, M., Schlag, P., Andres, S., Kleist, E., Mentel, T. F., Rohrer, F., Springer, M., Tillmann, R., Wildt, J., Wu, C., Zhao, D., Wahner, A., and Kiendler-Scharr, A.: Impact of NOx on secondary organic aerosol (SOA) formation from α-pinene and β-pinene photo-oxidation: the role of highly oxygenated organic nitrates, Atmos. Chem. Phys. Discuss., 2020, 1-40, 10.5194/acp-2019-1168, 2020.

Rohrer, F., Bohn, B., Brauers, T., Bruning, D., Johnen, F. J., Wahner, A., and Kleffmann, J.: Characterisation of the photolytic HONO-source in the atmosphere simulation chamber SAPHIR, Atmos. Chem. Phys., 5, 2189-2201, 2005.

Zhao, D. F., Buchholz, A., Kortner, B., Schlag, P., Rubach, F., Fuchs, H., Kiendler-Scharr, A., Tillmann, R., Wahner, A., Watne, Å. K., Hallquist, M., Flores, J. M., Rudich, Y., Kristensen, K., Hansen, A. M. K., Glasius, M., Kourtchev, I., Kalberer, M., and Mentel, T. F.: Cloud condensation nuclei activity, droplet growth kinetics, and hygroscopicity of biogenic and anthropogenic secondary organic aerosol (SOA), Atmos. Chem. Phys., 16, 1105-1121, 10.5194/acp-16-1105-2016, 2016.

Zhao, D. F., Schmitt, S. H., Wang, M. J., Acir, I. H., Tillmann, R., Tan, Z. F., Novelli, A., Fuchs, H., Pullinen, I., Wegener, R., Rohrer, F., Wildt, J., Kiendler-Scharr, A., Wahner, A., and Mentel, T. F.: Effects of NOx and SO2 on the secondary organic aerosol formation from photooxidation of alpha-pinene and limonene, Atmos. Chem. Phys., 18, 1611-1628, 10.5194/acp-18-1611-2018, 2018.

Supplement figures and tables

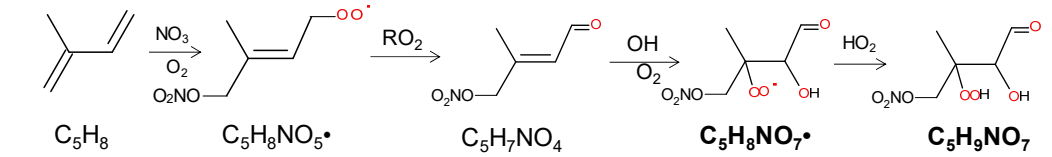

(a)

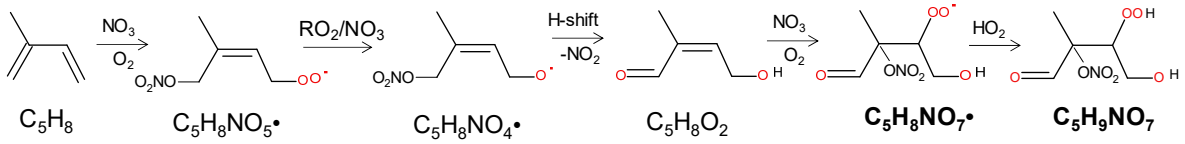

(b)

Scheme S1. The example pathway to form second-generation $C_5H_9NO_7$

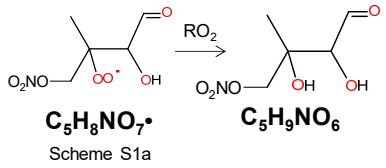

(a)

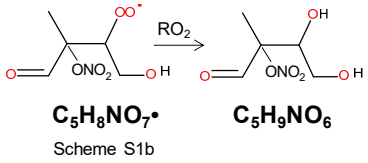

(b)

Scheme S2. The example pathway to form second-generation $C_5H_9NO_6$.

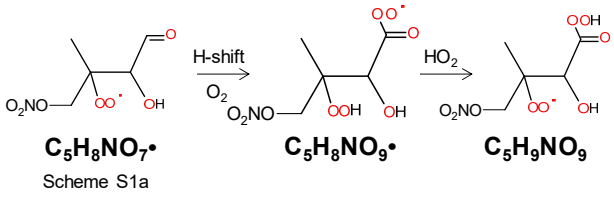

(a)

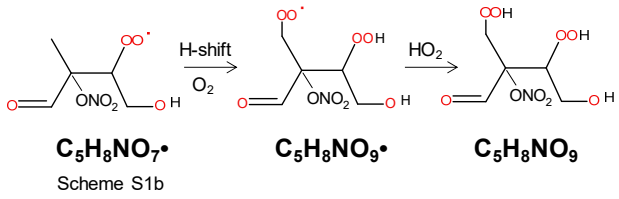

(b)

Scheme S3. The example pathway to form second-generation $C_5H_9NO_9$.

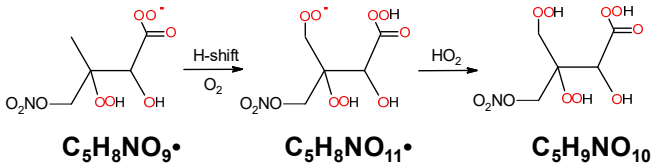

Scheme S3a

(a)

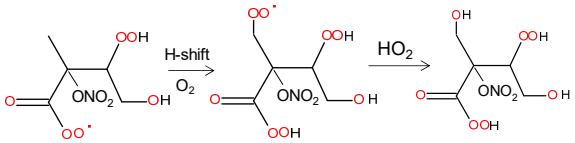

Scheme S3b

(b)

Scheme S4. The example pathway to form second-generation $C_5H_9NO_{10}$

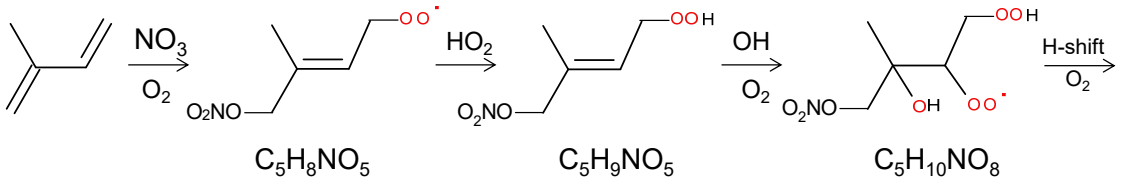

(a)

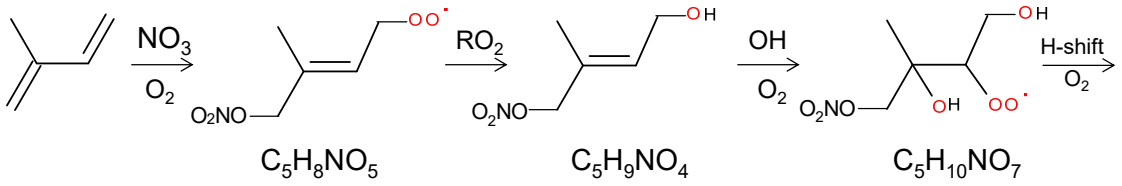

(b)

Scheme S5. The pathway to form $C_5H_{10}NO_{n(n\geq7)}$• RO_2 series with even (a) and odd (b) number of oxygen atoms.

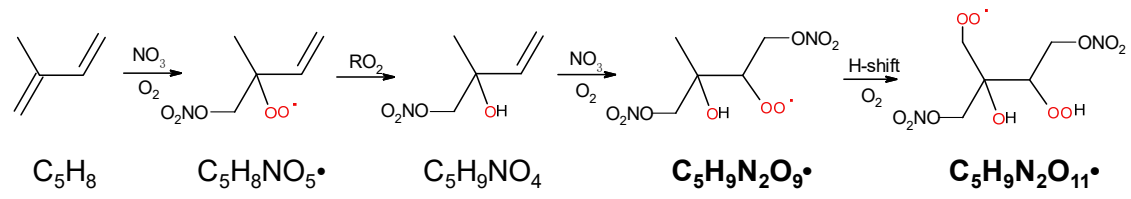

(a)

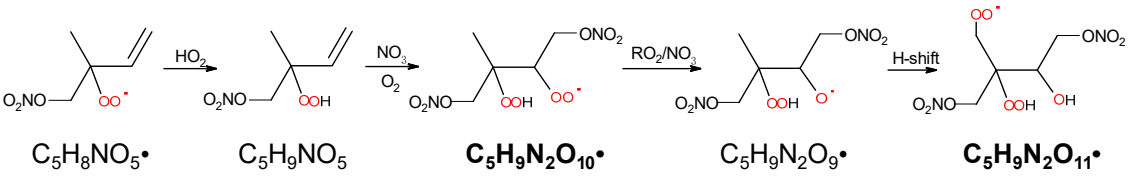

(b)

Scheme S6. The example pathway to form $C_5H_9N_2O_n$ (n=9, 11) HOM RO_2 series via 1-NO_3-isoprene-2-OO RO_2 by RO_2 channel (a) and alkoxy-peroxy channel. The detected products are in bold.

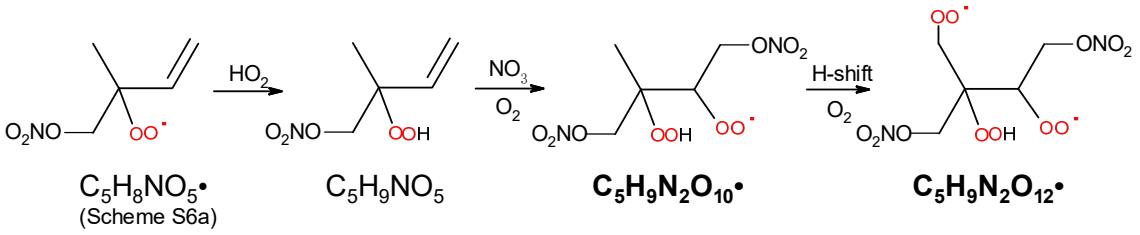

(a)

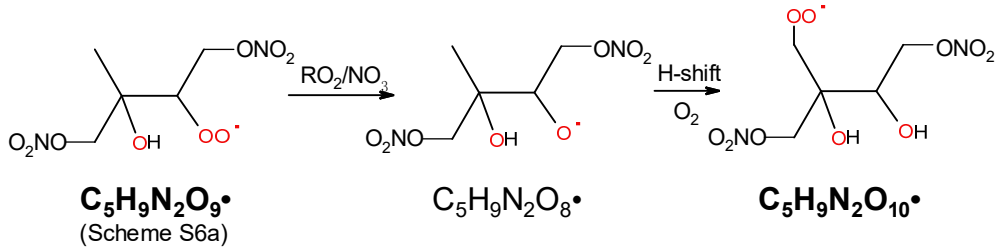

(b)

Scheme S7. The example pathway to form $C_5H_9N_2O_n$ (n=8, 10, 12) HOM RO_2 series via 1-NO_3-isoprene-2-OO RO_2 by RO_2 channel (a) and alkoxy-peroxy channel. The detected products are in bold.

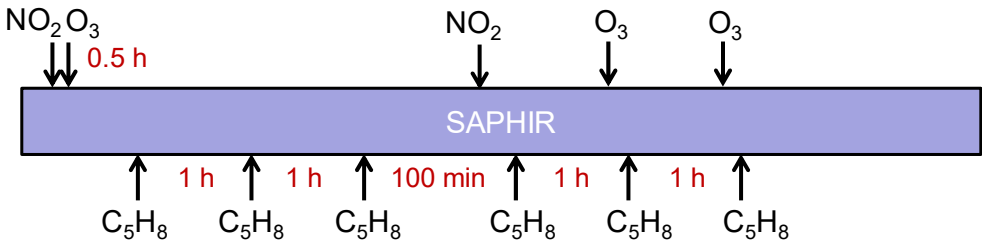

Figure S1. Schematic of the experimental procedure.

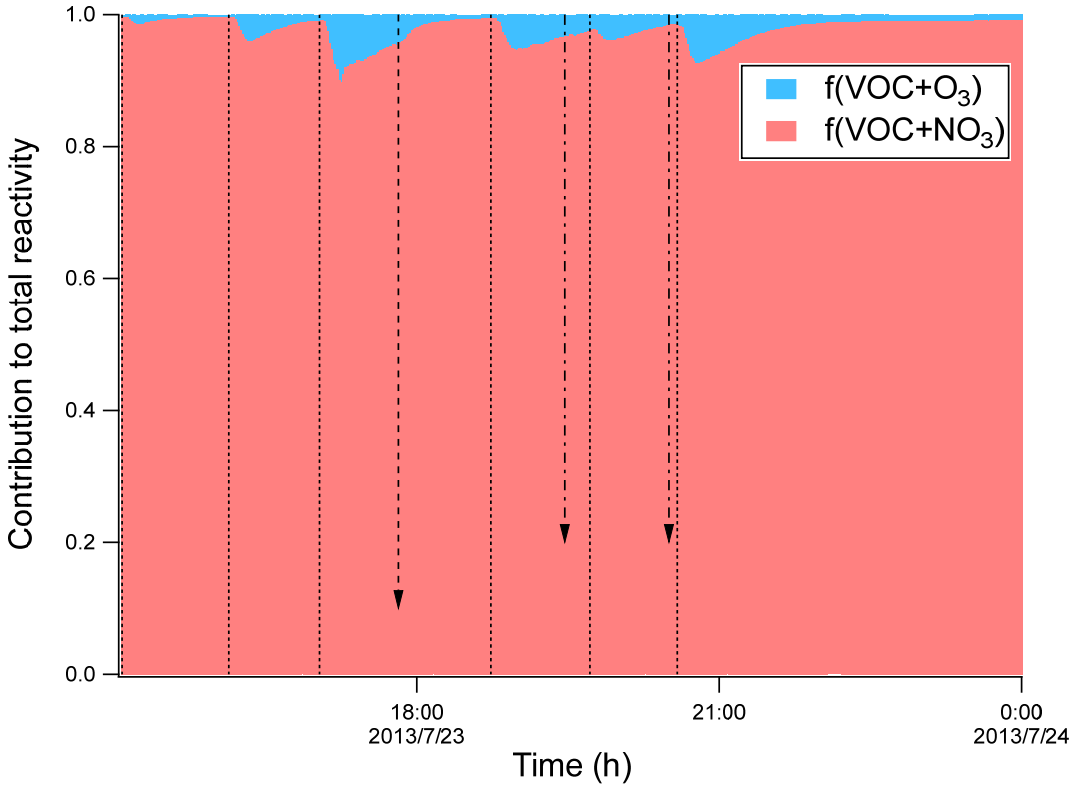

Figure S2. Relative contributions of the reaction rates of isoprene with NO_3 and with O_3 to the total isoprene loss. The dashed lines indicate the time of isoprene additions. The long-dashed arrow indicates the time of NO_2 addition. The dash-dotted arrows indicate the time of O_3 additions.

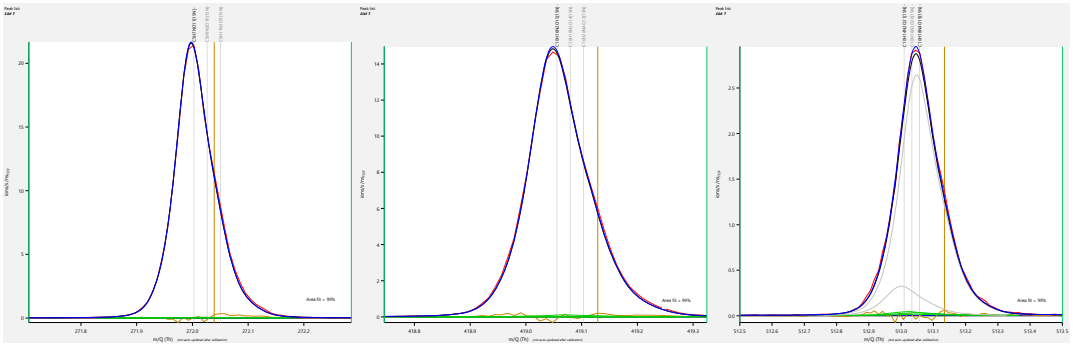

(a) (b) (c)

Figure S3. Examples of peak fitting. Formula in grey indicate compounds that have no noticeable effect on fitting residues and thus not included in the peak list.

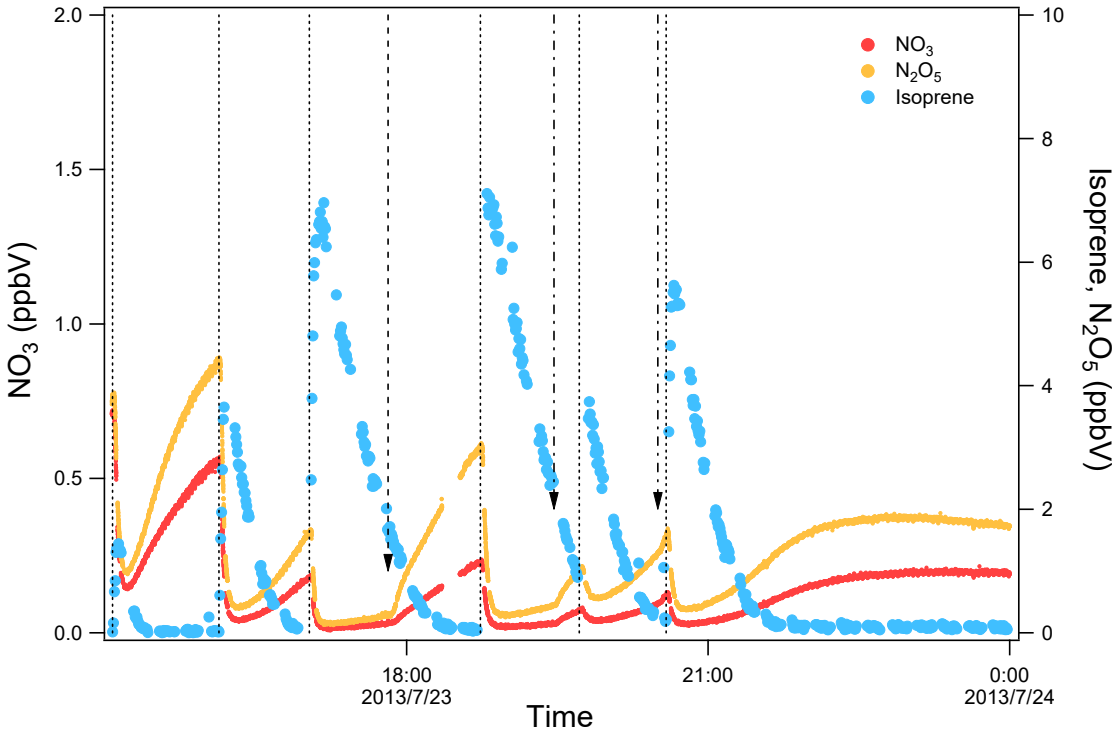

Figure S4. Time series of the of isoprene, NO_3, and N_2O_5 concentration. The dashed lines indicate the time of isoprene additions. The long-dashed arrow indicates the time of NO_2 addition. The dash-dotted arrows indicate the time of O_3 additions.

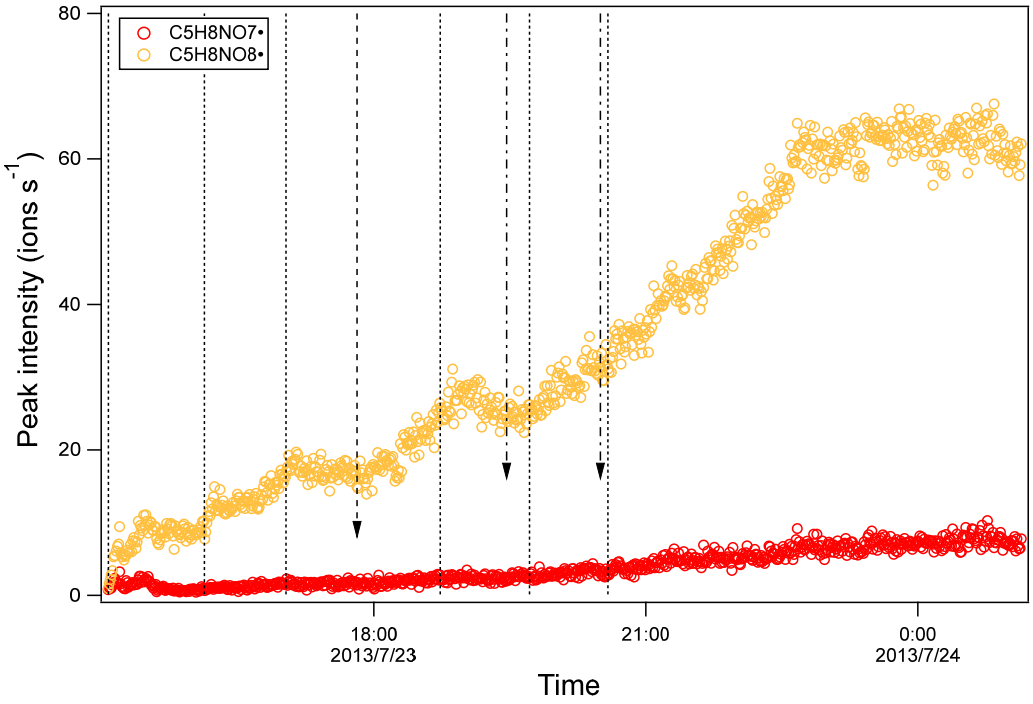

Figure S5. Time series of peak intensity of several HOM monomers of the $C_5H_8NO_n$• series. The dashed lines indicate the time of isoprene additions. The long-dashed arrow indicates the time of NO_2 addition. The dash-dotted arrows indicate the time of O_3 additions.

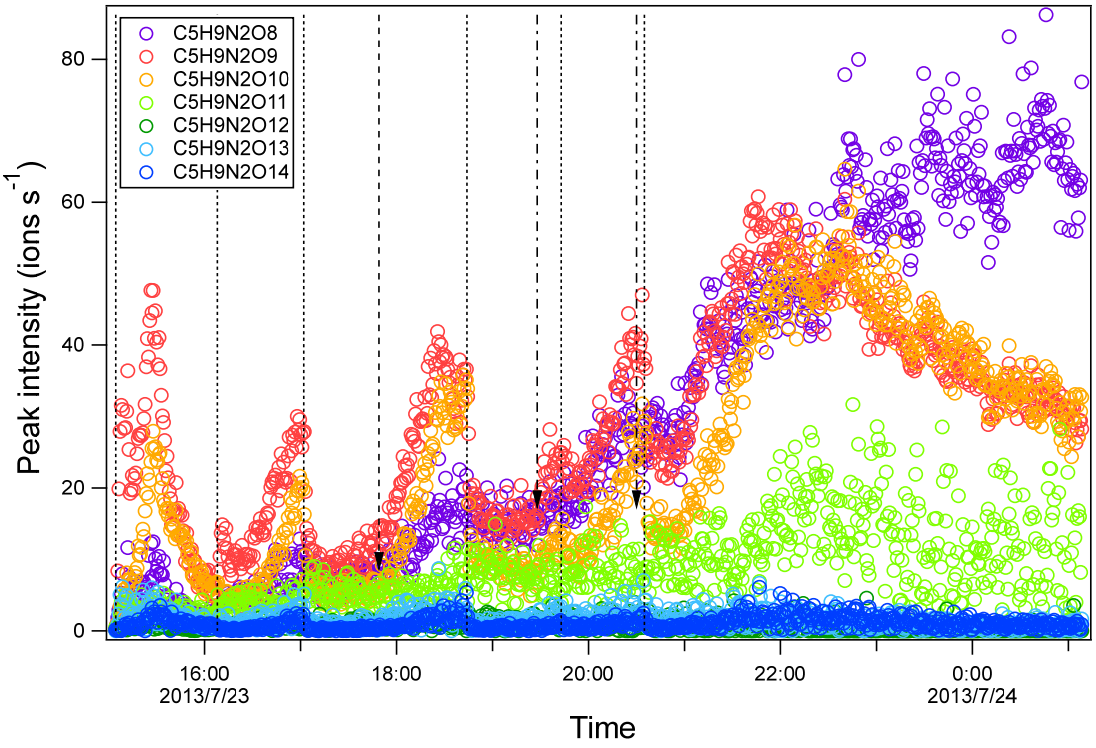

Figure S6. Time series of peak intensity of HOM monomers of the $C_5H_9N_2O_n$• series. The dashed lines indicate the time of isoprene additions. The long-dashed arrow indicates the time of NO_2 addition. The dash-dotted arrows indicate the time of O_3 additions.

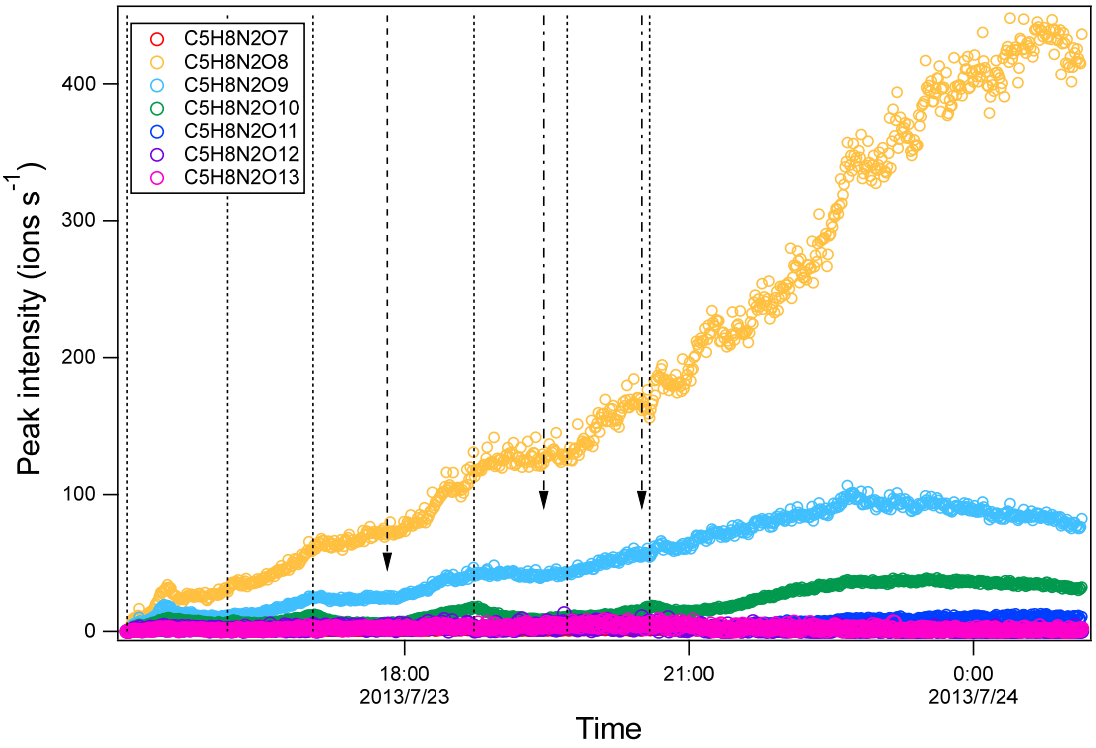

Figure S7. Time series of peak intensity of several HOM monomers of the $C_5H_8N_2O_n$ series (termination products of RO_2 $C_5H_9N_2O_n$). The dashed lines indicate the time of isoprene additions. The long-dashed arrow indicates the time of NO_2 addition. The dash-dotted arrows indicate the time of O_3 additions.

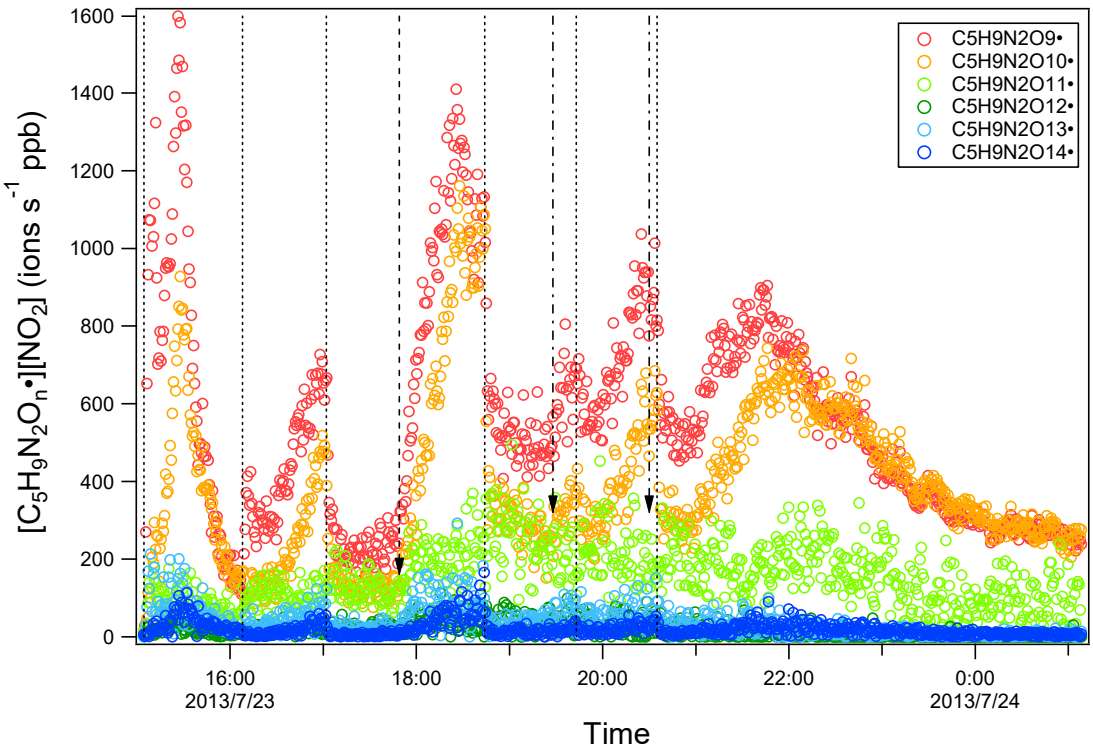

Figure S8. Time series of the product of the peak intensity of $C_5H_9N_2O_n$• and NO_2 concentration. The dashed lines indicate the time of isoprene additions. The long-dashed arrow indicates the time of NO_2 addition. The dash-dotted arrows indicate the time of O_3 additions.

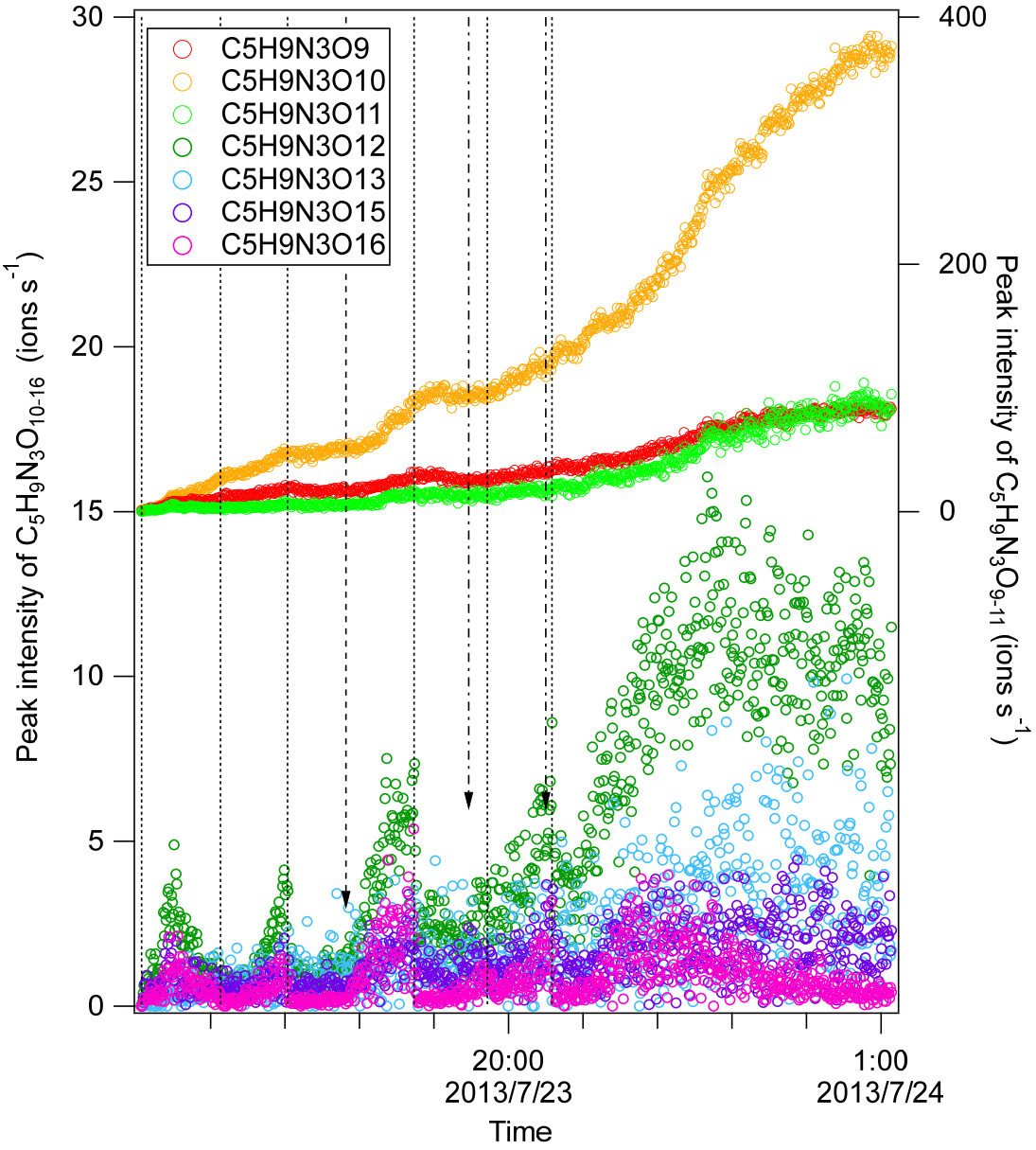

Figure S9. Time series of peak intensity of HOM monomers of the $C_5H_9N_3O_n$ series. The peak intensity of is shown on the left axis except for $C_5H_9N_3O_{10}$. The dashed lines indicate the time of isoprene additions. The long-dashed arrow indicates the time of NO_2 addition. The dash-dotted arrows indicate the time of O_3 additions.

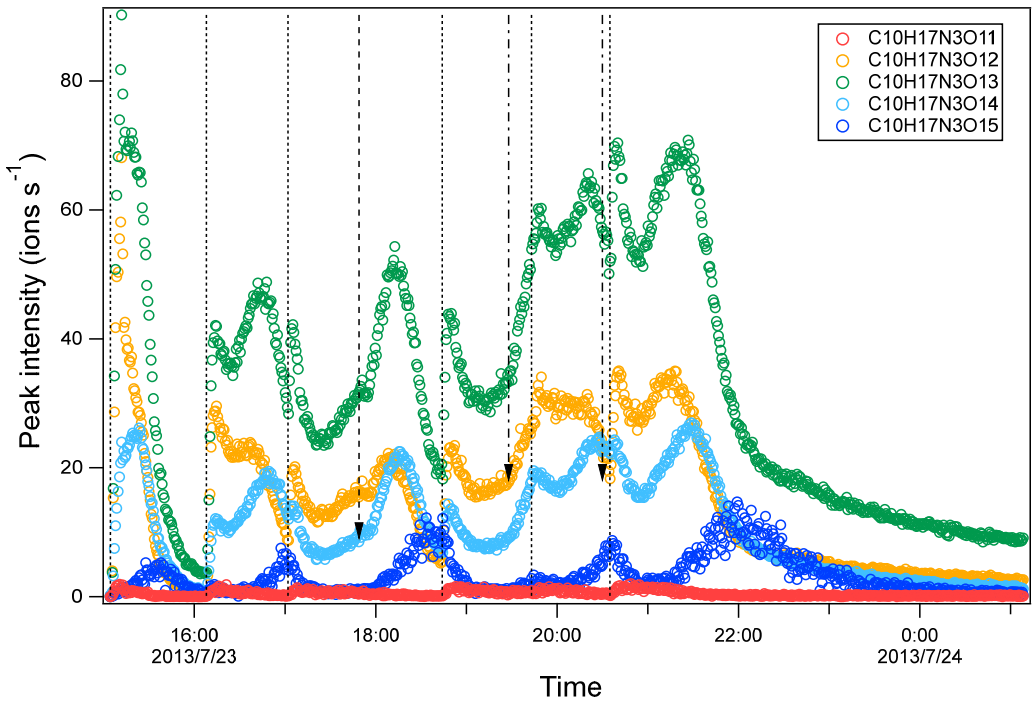

(a)

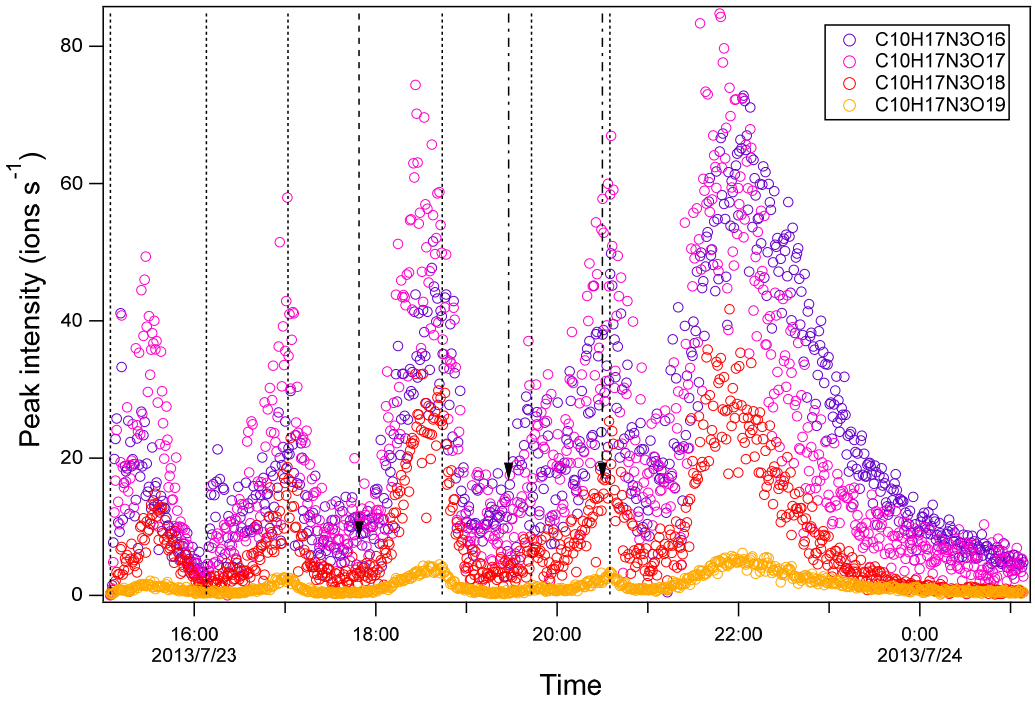

(b)

Figure S10. Time series of peak intensity of several HOM dimers of the $C_{10}H_{17}N_3O_n$ series for n=11-15(a) and 16-19 (b). The dashed lines indicate the time of isoprene additions. The long-dashed arrow indicates the time of NO_2 addition. The dash-dotted arrows indicate the time of O_3 additions.

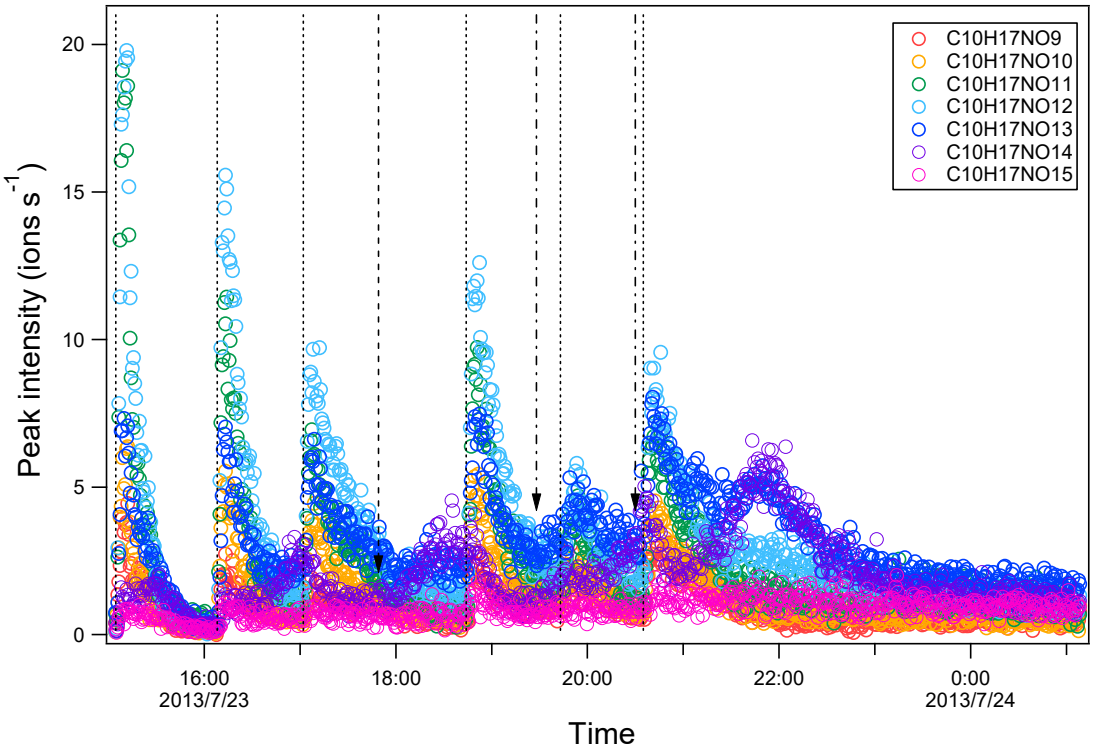

Figure S11. Time series of peak intensity of HOM monomers $C_{10}H_{17}NO_n$ series. The dashed lines indicate the time of isoprene additions. The long-dashed arrow indicates the time of NO_2 addition. The dash-dotted arrows indicate the time of O_3 additions.

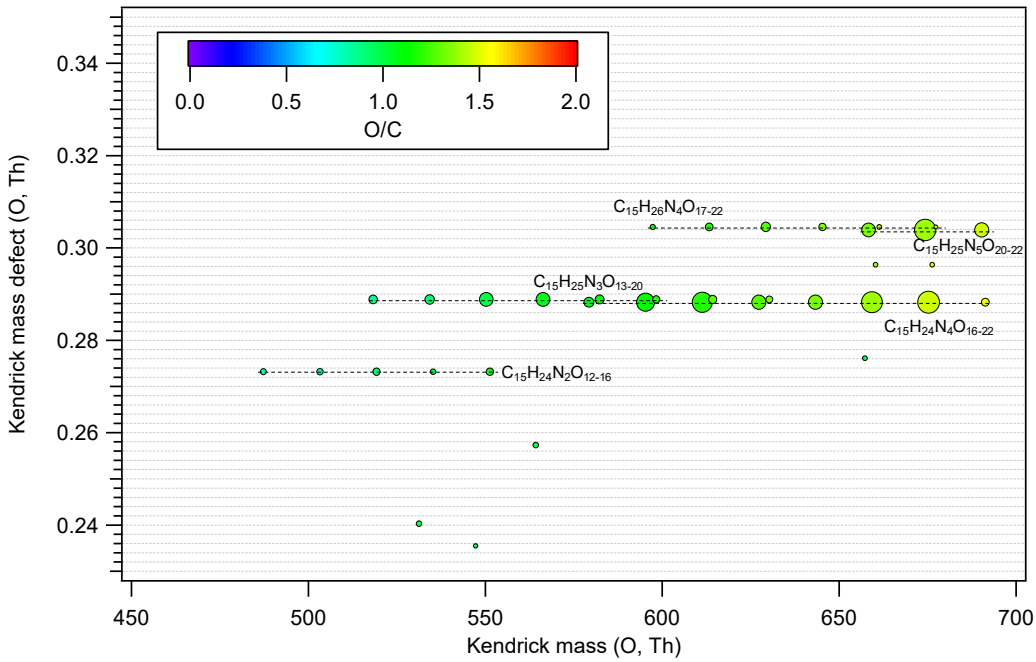

Figure S12. Kendrick mass defect with Kendrick base O of HOM trimers formed in isoprene+NO_3. The area of the circles is set to be proportional to the average peak intensity of each molecular formula during the first isoprene addition period (P1).

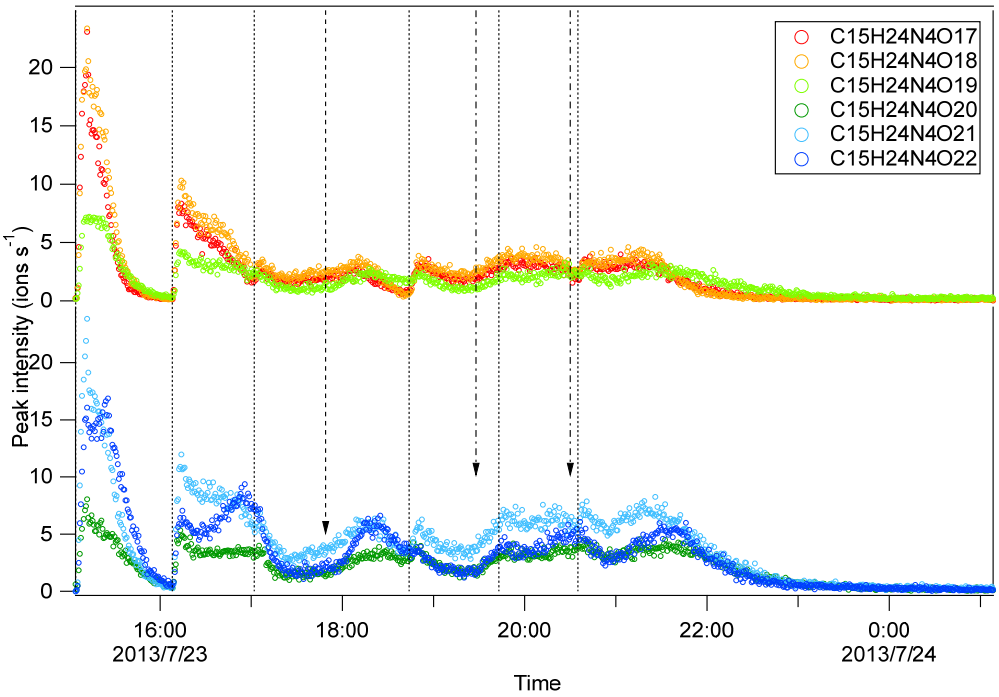

Figure S13. Time series of peak intensity of several HOM dimers of the $C_{15}H_{24}N_4O_n$ series. It is noted that the compounds are plotted in two panels for clarity. The dashed lines indicate the time of isoprene additions. The long-dashed arrow indicates the time of NO_2 addition. The dash-dotted arrows indicate the time of O_3 additions.

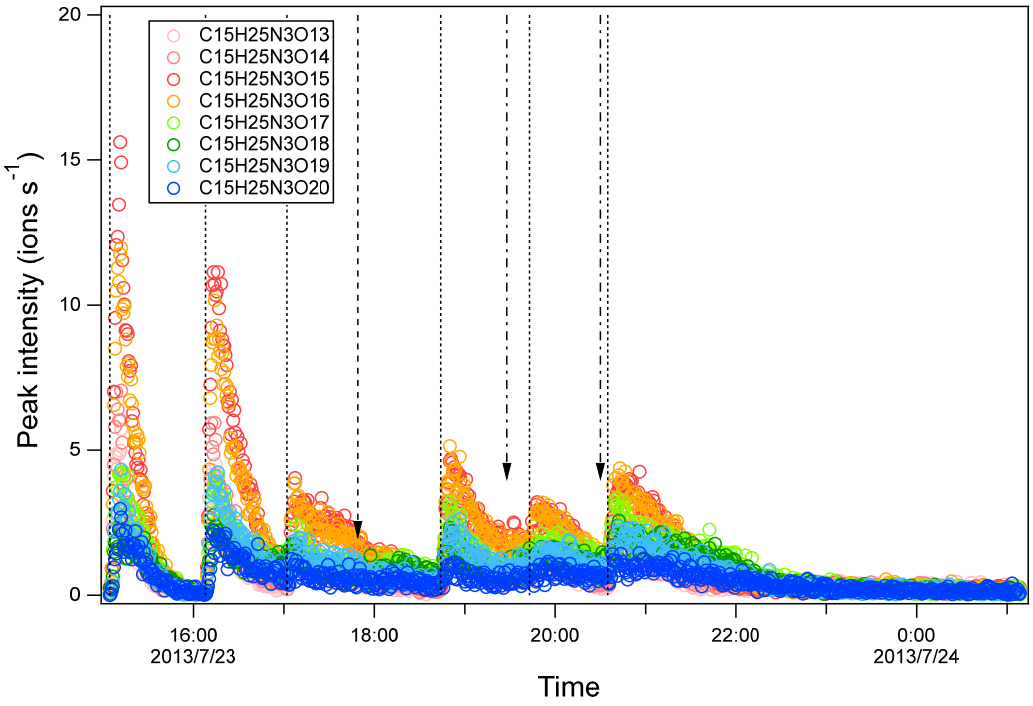

Figure S14. Time series of peak intensity of several HOM dimers of the $C_{15}H_{25}N_3O_n$ series. The dashed lines indicate the time of isoprene additions. The long-dashed arrow indicates the time of NO_2 addition. The dash-dotted arrows indicate the time of O_3 additions.

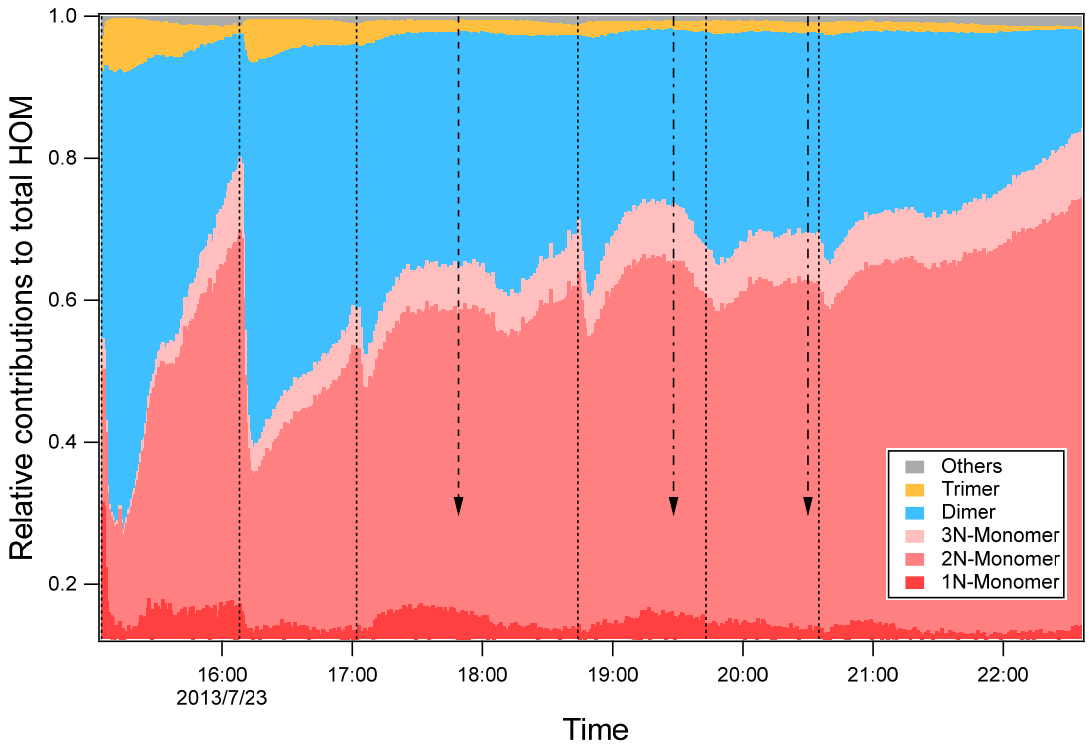

Figure S15. Relative contributions of HOM monomers, dimers, and trimers. Monomer 1-3N refers to the monomers containing 1-3 nitrogen atoms. The dashed lines indicate the time of isoprene additions. The long-dashed arrow indicates the time of NO_2 addition. The dash-dotted arrows indicate the time of O_3 additions.

Table S1. Intensity of HOM monomers $C_5H_8NO_n$ and their corresponding termination products.

Series	**Peroxy radical**	**Carbonyl**	**Hydroxyl**[c]	**Hydroperoxide**[c]	**Carbonyl**
m/z	**m**	**m-17**	**m-15**	**m+1**	**/Hydroxyl**
M1a	$C_5H_8NO_7$	$C_5H_7NO_6$	$C_5H_9NO_6$	$C_5H_9NO_7$	
	257.016	240.013	242.028	258.023	
	1.5%[a]	4.5%	2.5%	13.9%	1.8
M1b	$C_5H_8NO_8$	$C_5H_7NO_7$	$C_5H_9NO_7$	$C_5H_9NO_8$	
	273.010	256.008	258.023	274.018	
	9.7%	8.1%	13.9%	24.9%[c]	0.6
M1a	$C_5H_8NO_9$	$C_5H_7NO_8$	$C_5H_9NO_8$	$C_5H_9NO_9$	
	289.0053	272.0026	274.0182	290.0131	
	11.9%[b]	34.0%	24.9%	28.5%	1.4
M1b	$C_5H_8NO_{10}$	$C_5H_7NO_9$	$C_5H_9NO_9$	$C_5H_9NO_{10}$	
	305.000	287.998	290.013	306.008	
	22.2%[b]	8.3%	28.5%	5.8%	0.3
M1a	$C_5H_8NO_{11}$	$C_5H_7NO_{10}$	$C_5H_9NO_{10}$	$C_5H_9NO_{11}$	
	320.995	303.992	306.008	322.003	
	2.3%	3.0%	5.8%	2.0%	0.5
M1b			$C_5H_9NO_{11}$		
			322.003		
			2.0%		

[a]: The intensities are average intensity of each peak in MS during the first cycle (C1) normalized to the peak with the maximum intensity ($C_{10}H_{17}N_3O_{13}$).

[b]: These intensities may be subject to higher uncertainties due to the overlap with $C_5H_{10}N_2O_8$ and $C_5H_{10}N_2O_9$.

[c]: The relative contribution of HOM with hydroxyl or hydroperoxide cannot be differentiated and thus the total intensity is listed here.

Table S2. Intensity of HOM monomers $C_5H_9N_2O_n$ and their corresponding termination products.

Series	**Peroxy radical**	**Carbonyl**	**Hydroxyl**	**Hydroperoxide**	**Carbonyl /Hydroxyl**
m/z	**m**	**m-17**	**m-15**	**m+1**	
M2b	$C_5H_9N_2O_8$	$C_5H_8N_2O_7$		$C_5H_{10}N_2O_8$	
	288.021	271.019		289.029	
	5.6%[a]	1.3%		99.1%	1.6
M2a	$C_5H_9N_2O_9$	$C_5H_8N_2O_8$	$C_5H_{10}N_2O_8$	$C_5H_{10}N_2O_9$	
	304.0162	287.0135	289.0291	305.024	
	24.9%	57.9%	**99.1%**	82.3%	0.6
M2b	$C_5H_9N_2O_{10}$	$C_5H_8N_2O_9$	$C_5H_{10}N_2O_9$	$C_5H_{10}N_2O_{10}$	
	320.011	303.008	305.024	321.019	
	14.4%	29.7%	82.3%	9.3%	0.4
M2a	$C_5H_9N_2O_{11}$	$C_5H_8N_2O_{10}$	$C_5H_{10}N_2O_{10}$	$C_5H_{10}N_2O_{11}$	
	336.006	319.003	321.019	337.014	
	3.3%	18.3%	9.3%	0.4%	2.0
M2b	$C_5H_9N_2O_{12}$	$C_5H_8N_2O_{11}$	$C_5H_{10}N_2O_{11}$	$C_5H_{10}N_2O_{12}$	
	352.001	334.998	337.014	353.009	
	0.7%	2.5%	0.4%	4.3%	7.1

[a]: The intensities are the average intensities of each peak in MS during the first cycle (C1) normalized to the peak with the maximum intensity ($C_{10}H_{17}N_3O_{13}$).

[b]: The relative contribution of HOM with hydroxyl or hydroperoxide cannot be differentiated and thus the total intensity is listed here.

Table S3. Summary of the 50 major HOM peaks in the reaction of isoprene with NO_3

Detected mass (m/Q)	HOM mass (Da)	HOM Formula
256.008	193.022	C5H7NO7
258.023	195.038	C5H9NO7
272.003	209.017	C5H7NO8
273.010	210.025	C5H8NO8
274.018	211.033	C5H9NO8
287.013	224.028	C5H8N2O8
287.997	225.012	C5H7NO9
289.005	226.020	C5H8NO9
289.029	226.044	C5H10N2O8
290.013	227.028	C5H9NO9
303.008	240.023	C5H8N2O9
304.016	241.031	C5H9N2O9
305.000	242.015	C5H8NO10
305.024	242.039	C5H10N2O9
306.008	243.023	C5H9NO10
318.019	255.034	C5H9N3O9
319.003	256.018	C5H8N2O10
320.011	257.026	C5H9N2O10
321.019	258.034	C5H10N2O10
334.014	271.029	C5H9N3O10
351.006	224.028	C5H8N2O8
353.022	226.044	C5H10N2O8
367.001	240.023	C5H8N2O9
368.009	241.031	C5H9N2O9
369.017	242.039	C5H10N2O9
372.055	309.070	C10H15NO10
403.061	340.075	C10H16N2O11
405.076	342.091	C10H18N2O11
419.056	356.070	C10H16N2O12
434.067	371.081	C10H17N3O12
434.067	371.081	C10H17N3O12
435.051	372.065	C10H16N2O13
450.062	387.076	C10H17N3O13
451.046	388.060	C10H16N2O14
464.041	401.055	C10H15N3O14
466.056	403.071	C10H17N3O14
467.040	404.055	C10H16N2O15
482.051	419.066	C10H17N3O15
498.046	435.061	C10H17N3O16
498.059	371.081	C10H17N3O12
499.030	436.045	C10H16N2O17
513.057	450.072	C10H18N4O16
514.041	451.056	C10H17N3O17
514.054	387.076	C10H13N3O13
529.052	466.067	C10H18N4O17

530.036	467.051	C10H17N3O18
611.094	548.109	C15H24N4O18
659.079	596.093	C15H24N4O21
674.090	611.104	C15H25N5O21
675.074	612.088	C15H24N4O22